A μCT-based investigation of the influence of tissue modulus variation, anisotropy and inhomogeneity on ultrasound propagation in trabecular bone

Wenlei Pan[a,b], Yi Shen[b], G. Harry van Lenthe[a]

[a] Biomechanics Section, Department of Mechanical Engineering, KU Leuven (University of Leuven), 3001 Leuven, Belgium
[b] Department of Control Science and Engineering, Harbin Institute of Technology, Harbin, 150001,China

Email addresses:
Wenlei Pan, wenlei@hit.edu.cn
Yi Shen, shen@hit.edu.cn
G. Harry van Lenthe, harry.vanlenthe@kuleuven.be

Corresponding author
G. Harry van Lenthe
Biomechanics Section, Department of Mechanical Engineering
KU Leuven (University of Leuven)
3001 Leuven, Belgium
Tel: +32 16 32 2595
Fax: +32 16 32 8999
E-Mail: harry.vanlenthe@mech.kuleuven.be

Abstract

Ultrasound propagation is widely used in the diagnosis of osteoporosis by providing information on bone mechanical quality. When it loses calcium, the tissue properties will first decrease. However, limited research about the influence of tissue properties on ultrasound propagation have been done due to the cumbersome experiment. The goal of this study was to explore the relationships between tissue modulus (Es) and speed of sound (SOS) through numerical simulations, and to study the influence of Es on the acoustical behavior in characterizing the local structural anisotropy and inhomogeneity. In this work, three-dimensional finite element (FE) simulations were performed on a cubic high-resolution (15μm) bovine trabecular bone sample ($4\times4\times4\ mm^3$, BV/TV=0.18) mapped from micro-computed tomography. Ultrasound excitations of 50kHz, 500kHz and 2MHz were applied in three orthogonal axes and the first arriving signal (FAS) was collected to quantify wave velocity. In this study, a strong power law relationship between Es and SOS was measured with estimated exponential index β=2.08~3.44 for proximal-distal (PD), anterior-posterior (AP) and medial-lateral (ML), respectively (all $R^2 > 0.95$). For various Es, a positive dispersion of sound speed with respect to sound frequency was observed and the velocity dispersion magnitude (VDM) was measured. Also, with Es=15GPa in three orientations, the SOS in PD axis is 2009±120m/s, faster than that of AP (1762±106m/s) and ML (1798±132m/s) (f=2MHz) directions. Besides, the standard deviation of SOS increases with the sound frequency and the Es in all directions except for that at 50kHz. For the mechanical properties, the apparent modulus with certain Es was highest in the longitudinal direction compared with the transverse directions. It indicates that the tissue modulus combining with anisotropy and inhomogeneity has great influence on ultrasound propagation. Simulation results agree well with theoretical and experimental results.

***Keywords*: Cancellous bone, Tissue modulus, Anisotropy, Inhomogeneity, Ultrasound, Finite Element**

1. Introduction

One important application of quantitative ultrasound (QUS) is to provide noninvasive assessments of the bone parameters that affect bone strength [1][5][6]. Parameters of speed of sound (SOS)[1] [9][32] and broad-band ultrasound attenuation (BUA) [2][4] are now used for diagnoses of fracture risk in osteoporosis at several skeletal sites including calcaneus and femur. The correlation between these elastic wave parameters and the bone mechanical properties has been studied to make the QUS an alternative method of radiation in bone measurement.

Cancellous bone is a complex porous matrix with hierarchical structures of 10-500μm [3]. The ultrasound stress waves propagating in bone is influenced by the tissue morphology, which therefore provides sound techniques the ability of characterizing bone microstructures. However, the complicated and heterogeneous matrix of trabeculae make it difficult to develop a unique theoretical framework to model the sound propagation. Attempts have been made to establish numerical models by neglecting multiple and coherent scattering effects, such as binary mixture model, Faran cylinder mode and the weak scattering model [4]. These models have shown considerable success in predicting ultrasound scattering in cancellous bone, but is still debatable in revealing the mechanical properties. What's more, specific conditions such as the small acoustic properties contrast between trabecular and its fluid filler need to be satisfied. In addition to its complexity, the microarchitecture anisotropy and inhomogeneity have been confirmed through experimental and computational studies and it suggests that the anisotropic trabeculae will influence the acoustic properties of ultrasonic backscattering [5], velocity and attenuation [6].

Simulation and experimental methods have always been used for studying ultrasound propagation. However, among these studies, some contradict results are always found. For instance, the linear correlation between SOS and BV/TV in [7] is in contrast to the studies in [8], the relationships between ultrasound velocity and elasticity are also different between [9] and [10], the estimated sound velocity values in [11][12] are also much lower compared with [13][14]. Besides, because of the limited accuracy and precision of experimental measurements, and the uncertainty of the values for tissue material properties of cancellous bone, it is difficult to exactly model the sound propagation in trabeculae [4]. Due to these limitations, the use of ultrasound for assessing bone quality in clinical applications is limited.

Simulation approaches based on microstructural imaging method have been provided to be powerful alternatives for the investigation of the ultrasound propagation in cancellous bone and for the mechanical study of trabeculae microarchitecture. Among these approaches, micro-computed tomography (μCT) based finite element (μFE) [6][15] technique is widely used in quantifying bone mechanical properties. Voxel-based models are widely used as they allow for an easy and accurate representation of bone external and internal geometry [15]. The mechanical properties as obtained through such numerical models have shown excellent agreement with experimental observations.

In cancellous bone, the structural (apparent) modulus influences ultrasound propagation. However, the structural modulus depends on inherent architecture and tissue properties, of which the latter will first decrease with calcium loss (even before the apparent architecture changes). Also, due to the dependence on local structures, it is important to establish the inherent complex structure and taking in account the structure complexity. So in this work, we try to reveal how the tissue modulus variation influences the ultrasound propagation in anisotropic and inhomogeneous trabeculae. With the

increasing availability of parallel computers and large-scale solvers, 3D finite element (FE) simulation based on a high resolution micro-CT trabeculae model, which is a type of active and volumetric nondestructive technique [16], were performed. The dependence of SOS on mechanical properties, ultrasound velocity dispersion, bone anisotropy and inhomogeneity were studied.

2. Materials and Methods

Numerical simulations of bone anisotropy were studied by ultrasound propagation in three orthogonal anatomical orientations. Instead of idealized periodic structures [17], a μCT-based trabecular model was built from bovine cancellous bone, and the finite element [8][15] technique was used to simulate the ultrasound wave propagation. The building of trabecular model in FE consists of the following steps: reconstruct the trabeculae architecture through μCT slices; filter the grayscale images to partly remove the noise and isolated parts; segment the region of interest to calculate the trabeculae into 3-dimensional surface model; create and discretize the FE solid model and assign material properties; define the load and boundary conditions on the FE model.

2.1 Bone Specimens and μCT Imaging

Cube-shaped bone specimens were removed from the left bovine femoral heads (Fig. 1). One specimen from the central region with uniform bone tissue was visually selected and was filed parallel and smooth with the surfaces aligned along the direction of load-bearing. Three principle anatomical orientations, proximal-distal (PD), medial-lateral (ML) and anterior-posterior (AP) [6] were marked on the specimen surfaces. Before measurements, the specimen was defatted with Trichloroethylene and then dried.

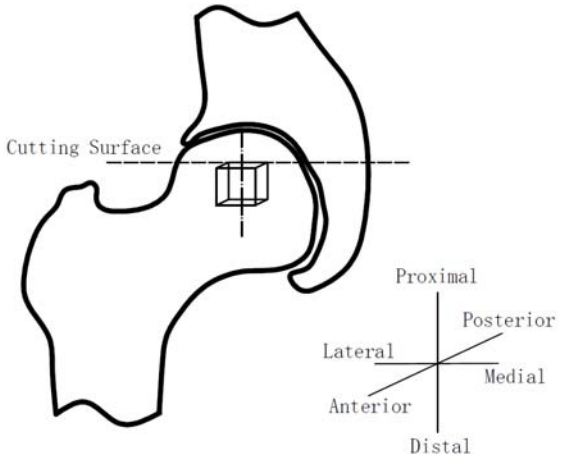

Fig. 1 Specimen preparation. Cube-shaped specimens were prepared from femoral heads with cube faces aligned along the pressure and tension directions of trabecular bone.

The 3-dimensional geometry of the bone sample was imaged by a Micro-CT system (μCT35, SCANCO Medical AG Inc., Brüttisellen, Switzerland) with nominal resolution of 15μm. The sample size was $4\times4\times4\ mm^3$ and had a BV/TV=0.18. The μCT images were converted to digital imaging and communications in medicine (DICOM) slices for later analysis on a 64-bit HP workstation (HP Integrity rx2800, Hewlett-Packard Development Company, L.P.). To filter the grayscale images, a median filter $(\sigma, 5\times5)$ [18]was used to reduce speckle noise and pepper noise, filter small holes and isolated parts and improve the model connectivity (Mathworks Inc., Natick, MA). The image segmentation was then performed by region growing and visually choosing the optimum threshold to include all trabeculae. The μCT image model and a slice cut from the model center are shown in Fig. 2.

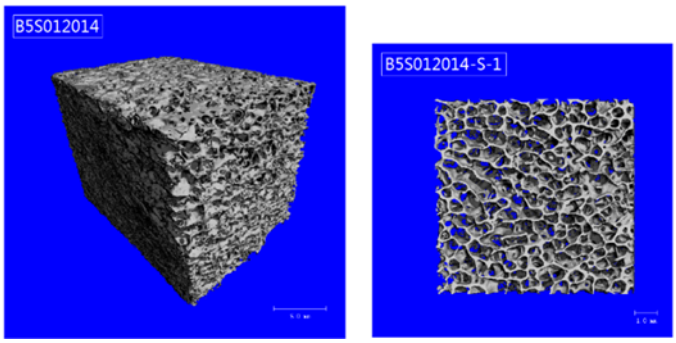

(A) (B)

Fig. 2: 3-dimensional μCT image of a trabecular bone model (A) and a slice cut from center of this model (B). The sample was imaged with nominal resolution of 15μm and had a BV/TV=0.18. Complex intrinsic structures can be observed.

2.2 Finite Element Simulation of Ultrasound Propagation in μCT-based Trabecular Model

The ultrasound propagation in elastic materials can be characterized by the elastic wave equation[19]

$$\left(\mu+\eta\frac{\partial}{\partial t}\right)\nabla^2\mathbf{u}+\left(\lambda+\mu+\xi\frac{\partial}{\partial t}\right)\nabla\nabla\cdot\mathbf{u}=\rho\frac{\partial\mathbf{u}^2}{\partial t^2} \tag{1}$$

where λ and μ are the first Lame parameter and the shear modulus parameter, t is the time and $\mathbf{u}=\mathbf{u}(x,y,z,t)$ is the time varying displacement vector with Cartesian coordinates x,$y$and z as the variables, $\eta$and ξrepresent the first and second viscosities respectively which were ignored in computing the wave propagation in our non-viscous model.

In simulations, ultrasound propagation in bone was modeled as the stress wave propagation, in which the wave velocity was computed as [19]:

$$V_L=\left(\frac{\lambda+2\mu}{\rho}\right)^{\frac{1}{2}} \qquad V_S=\left(\frac{\mu}{\rho}\right)^{\frac{1}{2}} \tag{2}$$

where V_L is the longitudinal velocity and V_S the shear velicity.

For ultrasound propagation, the FE technique was used to numerically solve the stress problems

[20] and the wave equation of (1)(2). The segmented masks were converted into a 3-dimensional surface model, which allows capture of complex geometrical structures. Then with the remesh function in Mimics, the surface model was transferred to solid FE model (Fig. 3) (Mimics V.16.0, Materialise NV, Leuven, Belgium), in which a mesh of linear brick elements, C3D8R, was created. The model, with elements number of 222,475 and node number of 322,497 was then imported into ABAQUS (ABAQUS 6.12, SIMULIA, Providence RI, USA). It should be noted that as the fluid phase of the bone sample has no influence on the fast wave propagation [8], in this work, there was no marrow included in the trabeculae model.

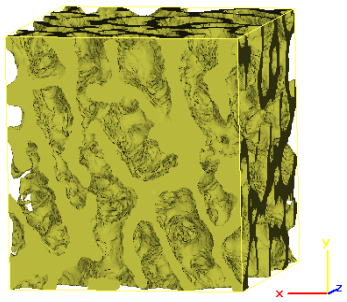

Fig. 3 The trabeculae surface model converted from segmented masks. No fluid marrow was included in this model. This model was then converted into solid model with element of C3D8R.

In the simulation, excitations at the tuned frequency of $f = 50\text{kHz}$, 500kHz and 2MHz were applied to the model along 3 orthogonal axes. Trabecular bone tissue was assumed to be linear elastic with the tissue density of 1962 kg/m^3 and the Poisson's ration of 0.3 [8]. A series of tissue modulus (Es) ranging from 500 MPa to 20 GPa were used to investigate the correlation between SOS and Es. Here the lower Es are much lower than previous research and are used as the reference values for estimating the variation trend of SOS. When solving the elastic wave equation, the density of discretization nodes should be at least 11 nodes per wave-length (i.e., $\lambda / L_N \geq 10$, where λ is the wave length and L_N is the average side length of elements) [21]. Therefore, in this work a mesh size of 45μm was used, which

resembles 1/20 of the wavelength at 2 MHz. Dynamic explicit analysis method was used and the stress wave was excited by introducing vibration boundary conditions, where a uniform sinusoidally varying ultrasound excitation with peak-peak vibration amplitude of 2μm was applied.

In this work, points of 6 uniformly distributed positions at the opposite side were selected (Fig. 4) and an early arriving signal, indicated as the first arriving signal (FAS) [22] was used for measuring the time of wave propagation. Once they were selected, in the following measurements (for separated axis) we always kept using these same points. The theoretical sound speed was calculated from the longitudinal wave formula [19], a transformation of (2) in anisotropic media with

$$V_{sos} = \sqrt{\mathrm{Es}(1-\nu)/\rho(1+\nu)(1-2\nu)} \tag{3}$$

where ρ is the tissue density and ν the poison ratio. For the simulation data, the coefficient and the exponential index in the power relationship between E_s and SOS, $Es=\alpha\times SOS^{\beta}$, was calculated through regression equations with least square method (LINEST).

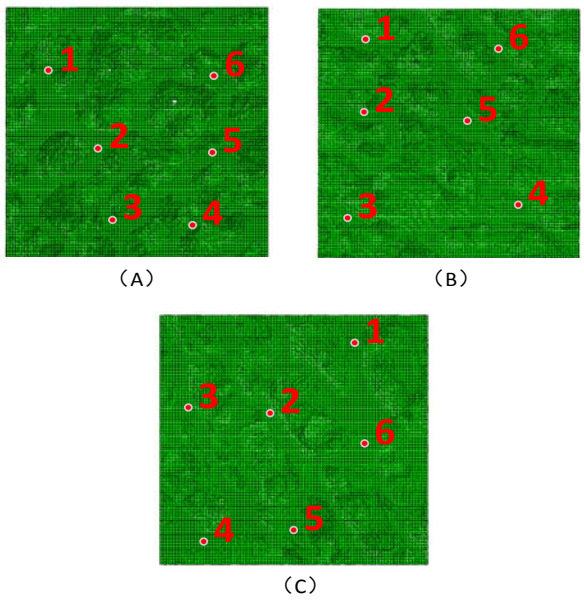

Fig. 4 Six points for measuring FAS in directions of PD (A), AP (B) and ML (C). These points were selected randomly with uniform distribution. In the following measurements (for separated axis) the same points were always used.

3. Results

One snapshot of the wave propagation at the ultrasound of 2MHz with Es=15GPa and one FAS in the ML direction were quantified (Fig. 5), demonstrating that the trabecular pathways affect ultrasound wave propagation (Fig. 5 (A)).

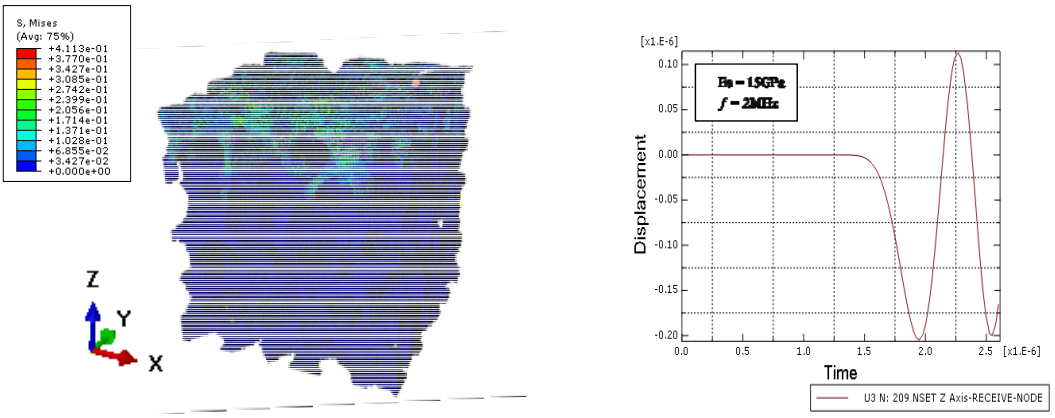

(A) (B)

Fig. 5 One snapshot of ultrasound wave propagation in μCT based trabecular model (A) and one of the observed FAS waveform propagating through this model (Es=15GPa, f=2MHz) in ML direction (B). The trabecular pathways show how sound waves propagates. The reversal amplitude of FAS is in favor of time marking.

The correlations between Es and SOS in three anatomical axes are shown in Fig. 6. The results suggest that there was a strong power law relationship between Es and SOS (Fig. 6) with exponential index ranging between 2.08~3.44 (all $R^2 > 0.95$). For ultrasound of 50kHz, 500kHz and 2MHz under different Es, the sound speed increases with the frequency in all anatomical axes (Fig. 6). For example, when Es=15GPa, the mean sound speed increases from 618m/s to 2009m/s, from 504m/s to 1762m/s, and from 552m/s to 1798m/s in PD, AP and ML directions respectively (Fig. 8). The ultrasonic dispersion is shown in Fig. 7. The standard deviations (SD) of measured sound speed (meters per second) at different points are summarized in Fig. 10. SD reveals the characteristics of bone

inhomogeneity and it increases with Es from 0.5GPa to 20GPa except for the $f = 50\text{kHz}$. Also, in our simulation the ultrasound with higher frequency shows to be more sensitive to the bone inhomogeneity than that of low frequency. For example, for $f = 2\text{MHz}$ in PD and ML direction, the standard deviations of SOS are 138.5m/s and 138.3m/s, higher than those of 118.3m/s and 90.0m/s at 500kHz. However, this pattern is not obvious in the AP axis. What's more, in this simulation the SOS in PD direction was measured higher than SOS in the other two directions (Fig. 8), which corresponds to the higher stiffness in the PD direction. In the three anatomical orientations, PD axis had an apparent modulus of 1600MPa, while for AP and ML axes, they were 1212MPa and 1379MPa (Fig. 9).

4. Discussion

Cancellous bone is a kind of structure with pillar trabeculae aligning along the principle (load bearing) axis. When bone losing its mineral density (BMD), the tissue properties will change and the porosity matrix will turn into sparse structures, which as a result changes the microarchitecture stiffness (for which, the trabeculae are the supporting pillars) and ultrasound velocity (for which, the trabeculae serve as the wave paths). Because without taking in account of the structural information, tissue properties cannot fully explain the variance in bone strength [23]. So in this work, we conducted research of the influence of tissue modulus combing with structure anisotropy and inhomogeneity on ultrasound propagation.

In the current study, the Es and SOS was measured to be of a strong power law relationship (Fig. 6) and the acoustic dispersion in bone was observed in three anatomical axes. This relationship agrees well with the general pattern in solid given by the Hooke's Law $V_{sos} = \sqrt{Es/\rho}$. This power law may be quantified with a number of different equation forms depending on what wave types are involved. When longitudinal stress waves are generated, the poison ration will be included as (3). In this

simulation, the estimated exponential index ranges between $\beta=2.08 \sim 3.44$, and the estimated exponential index indicate that the longitudinal wave equation ($\beta'=2$) is better approximated when using higher frequencies (Fig. 6).

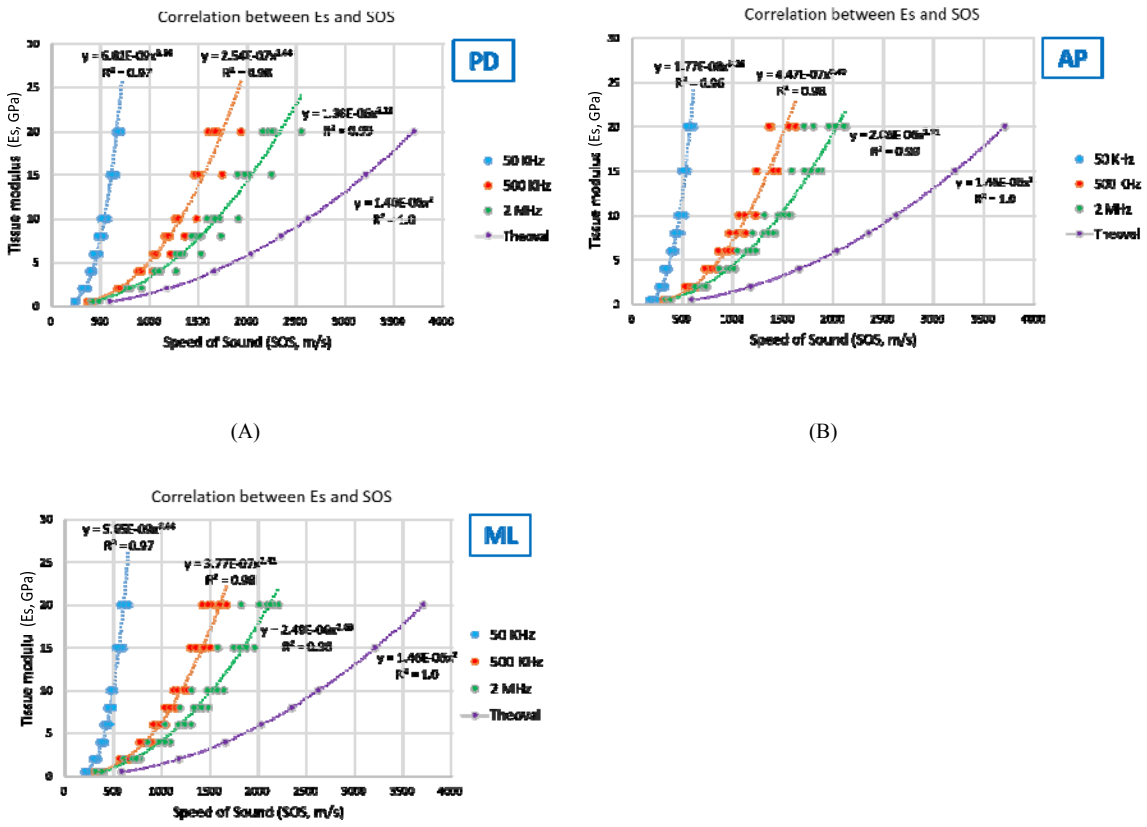

(A) (B)

(C)

Fig. 6 Correlations between the SOS and the tissue modulus Es in three orientations of PD (A), AP (B) and ML (C) with FE simulations. Ultrasound frequencies of 50kHz, 500kHz and 2MHz were investigated with Es ranging from 0.5GPa to 20GPa. The longitudinal wave speed formula (presented in the context) is given as a reference.

This work can explain the dispersive characteristics of bone as a consequence of the trabecular microstructure. Acoustic dispersion happens with ultrasound waves separating into component frequencies when the front waves pass through the bone microstructure. This microarchitecture involves different mechanisms of scattering and mode conversion that will interfere with each other at

certain frequencies and then contribute to the dispersion. Even though lots of work on acoustic dispersion in bone has been done, limited theoretical development has been advanced so far. In this research, the velocity dispersion magnitude (VDM) [24] was used to characterize the velocity dispersion. VDM is defined as $\mathrm{VDM} = \Delta V = V(f_{max}) - V(f_{min})$ where f_{min} and f_{max} are the limits of frequency bandwidth. Table 1 shows the VDM at different Es values. For ultrasound of 50kHz, 500kHz and 2MHz and Es=15GPa, the VDM was 1390.4m/s, 1257.6m/s and 1244.9m/s in PD, AP and ML directions respectively (Table 1). This is much larger than the VDM (< 56m/s) measured by [25] in a narrower frequency bandwidth of 50kHz~200kHz and the VDM (~120m/s) by [24] in 200kHz~600kHz. It should also be noted that when sound propagates through the roughly rod and pillar-shaped trabeculae, the porous structure and the twist trabecular paths result in a reduced SOS in simulations compared with that calculated from the longitudinal wave formula (Fig. 6).

Table 1. Velocity dispersion magnitude (VDM, m/s) of different tissue modulus under ultrasound frequency of 50 kHz to 2 MHz in three orientations.

Es (GPa)	PD direction	AP direction	ML direction
0.5	181.29	160.25	149.24
2	470.82	407.01	401.18
4	719.55	622.90	612.10
6	901.44	759.67	774.51
8	1040.74	890.82	916.84
10	1162.06	1007.14	1040.37
15	1390.40	1257.60	1244.93
20	1607.76	1388.36	1448.93

In addition, positive dispersion was observed under different tissue modulus, i.e. increased speed of sound as frequency increased. Fig. 7 shows the dispersion in representative direction of ML with Es=4GPa (A), 8GPa (B) and 15GPa (C). ML is the common direction used for clinical diagnosis. Related results can be found in previous research. In Droin's research [24], the velocity dispersion of cancellous bone showed to be either negative or positive in the frequency of 200kHz to 600kHz. Then in a wider frequency range covering 0.3~3MHz, positive dispersion was found, which agrees with the results in this paper. Similar positive dispersion results were also found in skull diploe [26], in cancellous bone [27] and in tissue-like polymers [28]. However, it is interesting that negative velocity dispersion was also found by some studies, such as the research in [29] and [30]. Then in [31], Christian et.al. presented both illustrations of dispersion observed in cancellous bone (negative) and the dispersion curve predicted by the causality-imposed Kramers-Kronig relations (positive). These conflicting findings imply the poor understanding of the mechanism of dispersion in cancellous bone.

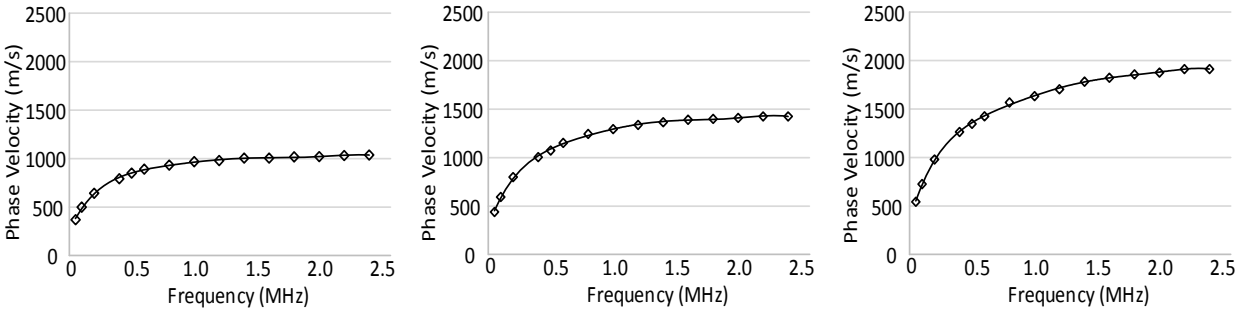

(A) (B) (C)

Fig. 7 Ultrasound dispersion in representative direction of ML with Es=4GPa (A), 8GPa (B) and 15GPa (C). ML direction is the direction normally used for clinical diagnosis in vivo.

In this simulation, the ultrasound propagation were measured in all three axes, and with various Es values, the calculated SOS in PD direction is higher than those in AP and ML directions (Fig. 8). For example, along PD axis, at frequency of $f = 2\mathrm{MHz}$ (Es=15GPa) the SOS is 2009±120m/s, while in AP and ML directions they are1762±106 and 1798±132m/s respectively. Similar SOS differences were

found in [32], and when the propagation angle θ to the main trabecular alignment ranging from 0 to $\pi/2$, the SOS was measured as a continuous function and decreased by 500m/s [33]. Since the acoustic anisotropy parallels the structural anisotropy [34], this significant difference between the SOS in different directions reveals the anisotropy of trabeculae arrangement. For instance, the experimental results on the acoustic anisotropy in bovine cancellous bone showed that the fast and slow longitudinal waves were in relation to the structural anisotropy [33]. Then in [35], the mechanical anisotropy of osteoporotic cancellous bone was further verified through a total of 82 cubic specimens. In some latest research [5][36], the anisotropy on stiffness and ultrasonic backscatter were also mentioned. These research have shown similar results as the acoustical and structural anisotropy shown in this paper. In this paper, the cancellous bone anisotropy revealed by mechanical property of stiffness is shown in Fig. 9. In the transverse directions, the apparent modulus Eapp (1212MPa for AP and 1379MPa for ML) are simulated much lower than that of PD direction (1600MPa), which agrees with the results in [8]. The trabecular system in cancellous bone, especially the fabric anisotropy [36] are believed to dominantly contribute to this stiffness anisotropy.

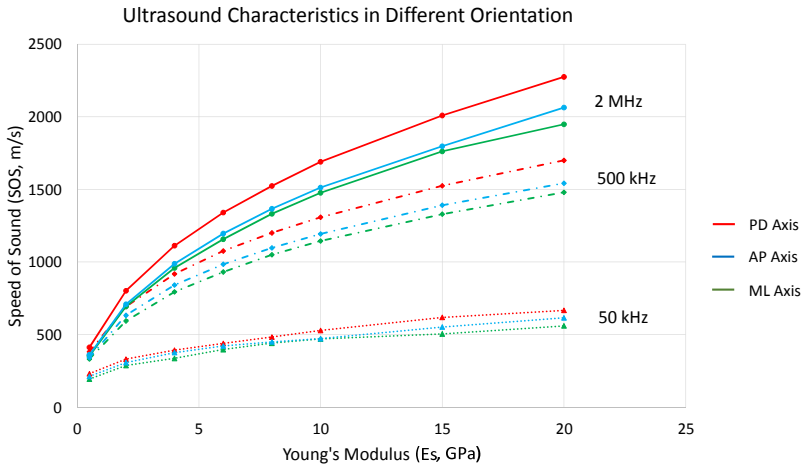

Fig. 8 Ultrasound velocities in different anatomical orientations measured through simulations. With various Es values, the calculated SOS in PD direction is higher than those in AP and ML directions. For the transverse directions AP and ML, SOS is almost the same.

FAS was used to measure the transmission time of ultrasound front wave, however in an inhomogeneous media, the distribution of the trabecular thickness and structural free-ends will make the acoustic field undergo a series of reflections and transmissions, and the front wave shape changes with different parts of the wave propagating at different speeds. Therefore the speed deviation of FAS (Fig. 10) determined by the structural deviations reveals the cancellous bone microarchitecture inhomogeneity. Previous research have shown the transverse inhomogeneity of bone by verifying regional variations with dual-energy computed tomography [37]. Other published data showed that almost all structural parameters are strongly dependent on the measurement location [38], and the mineralization variation and the morphology difference contributes a lot to this inhomogeneity [39]. In this work, it shows that the standard deviation of sound speed σ measured at different points increases with the frequency f (Fig. 10), and positive correlations between SD and Es were found except for the sound at $f = 50\text{kHz}$. This increased SD implies more efficiency of sound with higher frequency in characterizing the structure inhomogeneity.

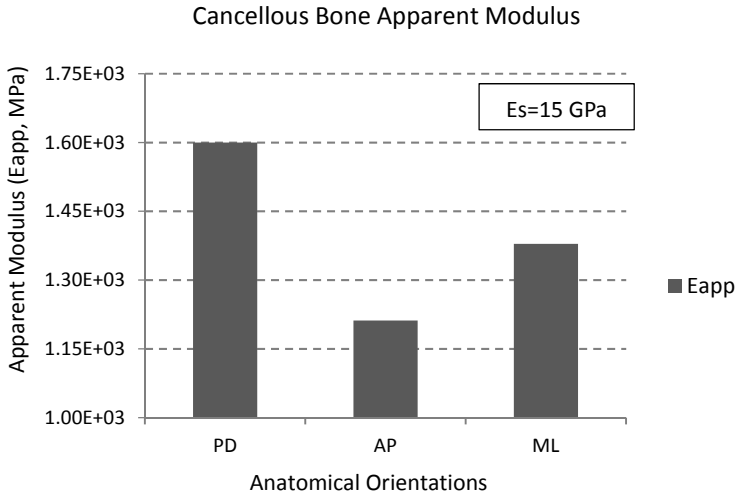

Fig. 9 Cancellous bone stiffness in 3 anatomical orientations with Es=15GPa. The apparent modulus Eapp in the transverse directions (1212MPa for AP and 1379MPa for ML) are simulated much lower than that of PD direction (1600MPa).

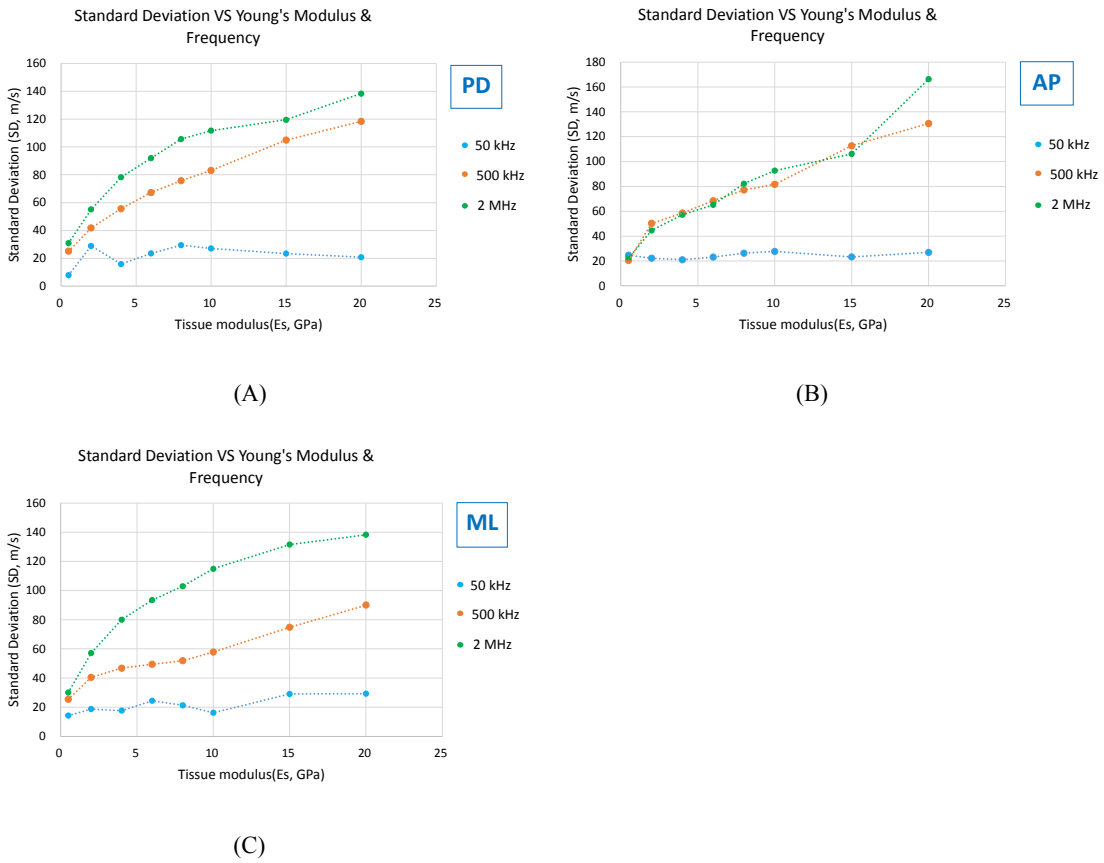

Fig. 10 Standard deviation of SOS from simulations with respect to frequency and Es. A positive correlation between SD and Es is shown except for the sound at $f = 50\text{kHz}$. Ultrasound with higher frequency shows more potential in characterizing the structure inhomogeneity.

Unlike experimental approaches, simulation in this work allows the exploration of independent varying parameters Es clarifying the physics of ultrasound propagation in extreme conditions. It was shown to be a comprehensive method for the study of micromechanical wave propagation, bone strength assessment and orthopaedics, especially to solve some physics problems that cannot be solved or observed through in vivo measurements. However, for numerical simulation there are disadvantages as well. First, substantial time and computer memory are required to complete the finite computation. Also, in calculating SOS, the choice of proper element size and the definition of boundary conditions for ultrasound propagation plays a crucial role. To exactly define these conditions, experiments and

pre-test on simplified models are needed. It should also be noted that in this work we were not making statistical computations of sample diversity, only one specimen was used for study to make the tissue modulus the only variable of our simulations. We keep simulating on the same trabeculae structures, and base on a constant trabeculae pattern, we performed research with a wide range of tissue values (0.5GPa~20GPa) (even lower or higher than its normal value) to make enough simulations to obtain reliable data.

5. Conclusion

In this work we have performed simulations of sound propagations at different frequencies with 3D real trabecular bone microarchitecture reconstructed from Micro CT. The cancellous bones were cut from bovine femoral heads, and the influences of tissue modulus on ultrasound propagation and the acoustical behavior in characterizing the local structural anisotropy and inhomogeneity under gradual tissue modulus were studied.

It indicates that between tissue modulus and speed of sound there is a strong power law relationship. This relationship is found in all three anatomical axes and agrees well with the general pattern of Hooke's Law. And it indicates that with higher frequencies, the power law estimation is more likely to reach the theoretical results. Also, with different Es values, positive ultrasonic dispersion i.e. increased speed of sound as frequency increased in bone is observed, which is in agreement with research conducted in a wide frequency rage. For wave propagation, in the proximal-distal direction it is faster than the other two directions; the same result is found for the stiffness. Then the capacity of ultrasound in assessing the bone microarchitecture inhomogeneity under various Es is presented by the speed deviation of FAS and it shows that the sensitivity improved with increasing frequency and tissue modulus. The results show that ultrasound simulation through computational models is an alternative to

experimental research and that it can effectively quantify the influence of tissue modulus on wave propagation in anisotropic and inhomogeneous trabeculae bone.

References

[1] Van den Bergh J P W, Van Lenthe G H, Hermus A, et al. Speed of sound reflects Young's modulus as assessed by microstructural finite element analysis[J]. Bone, 2000, 26(5): 519-524.

[2] Moayyeri A, Adams J E, Adler R A, et al. Quantitative ultrasound of the heel and fracture risk assessment: an updated meta-analysis[J]. Osteoporosis International, 2012, 23(1): 143-153.

[3] Allena R, Cluzel C. Identification of anisotropic tensile strength of cortical bone using Brazilian test[J]. Journal of the mechanical behavior of biomedical materials, 2014, 38: 134-142.

[4] Wear K A. Ultrasonic scattering from cancellous bone: a review[J]. Ultrasonics, Ferroelectrics, and Frequency Control, IEEE Transactions on, 2008, 55(7): 1432-1441.

[5] Liu C, Ta D, Fujita F, et al. The relationship between ultrasonic backscatter and trabecular anisotropic microstructure in cancellous bone[J]. Journal of Applied Physics, 2014, 115(6): 064906.

[6] Lin L, Oon H Y, Lin W, et al. Principal trabecular structural orientation predicted by quantitative ultrasound is strongly correlated with uFEA determined anisotropic apparent stiffness[J]. Biomechanics and modeling in mechanobiology, 2014, 13(5): 961-971.

[7] Haiat G, Padilla F, Laugier P. Sensitivity of QUS parameters to controlled variations of bone strength assessed with a cellular model[J]. IEEE Transactions on Ultrasonics Ferroelectrics and Frequency Control, 2008, 55(7): 1488-1496.

[8] Goossens L, Vanderoost J, Jaecques S, et al. The correlation between the SOS in trabecular bone and stiffness and density studied by finite-element analysis [J]. Ultrasonics, Ferroelectrics, and Frequency Control, IEEE Transactions on, 2008, 55(6): 1234-1242.

[9] Hans D, Wu C, Njeh C F, et al. Ultrasound velocity of trabecular cubes reflects mainly bone density and elasticity[J]. Calcified tissue international, 1999, 64(1): 18-23.

[10] Goossens L, Vanderoost J, Jaecques S V N, et al. Microstructural simulation of ultrasonic wave propagation through vertebral bone samples[C]//Ultrasonics Symposium, 2008. IUS 2008. IEEE. IEEE, 2008: 142-145.

[11] Haiat G, Padilla F, Peyrin F. Variation of Ultrasonic Parameters With Microstructure and Material Properties of Trabecular Bone: A 3D Model Simulation[J]. Journal of Bone and Mineral Research, 2007, 22(5): 665-674.

[12] Chaffai S, Peyrin F, Nuzzo S. Ultrasonic characterization of human cancellous bone using transmission and backscatter measurements: relationships to density and microstructure[J]. Bone, 2002, 30(1): 229-237.

[13] Nicholson P H F, Haddaway M J, Davie M W J. The dependence of ultrasonic properties on orientation in human vertebral bone[J]. Physics in medicine and biology, 1994, 39(6): 1013.

[14] Hosokawa A, Otani T. Ultrasonic wave propagation in bovine cancellous bone[J]. Journal of the Acoustical Society of America, 1997, 101(1): 558-562.

[15] Torcasio A, Zhang X, Van Oosterwyck H. Use of micro-CT-based finite element analysis to accurately quantify peri-implant bone strains: a validation in rat tibiae[J]. Biomechanics and Modeling in Mechanobiology, 2011, 11(5): 743-750.

[16] Tapfer A, Bech M, Zanette I. Three-dimensional imaging of whole mouse models: comparing nondestructive X-ray phase-contrast micro-CT with cryotome-based planar epi-illumination imaging[J]. Journal of Microscopy, 2014, 253(1): 24-30.

[17] Goda I, Ganghoffer J F. Identification of couple-stress moduli of vertebral trabecular bone based on the 3D internal architectures[J]. Journal of the mechanical behavior of biomedical materials, 2015, 51: 99-118.

[18] Ravi Kishore T, Deergha Rao K. Efficient median filter for restoration of image and video sequences corrupted by impulsive noise[J]. IETE Journal of Research, 2010, 56(4): 219-226.

[19] Achenbach J. Wave propagation in elastic solids[M]. Elsevier, 1984

[20] Buchkremer S, Klocke F, Lung D. Finite-element-analysis of the relationship between chip geometry and stress triaxiality distribution in the chip breakage location of metal cutting operations[J]. Simulation Modelling Practice and Theory, 2015, 55: 10-26.

[21] Pan W, Shen Y, Liu T, et al. Stress Estimation in Different Bone Layers Subject to Therapeutic Ultrasound in an Intelligent Bone System[J]. Instrumentation and Measurement, IEEE Transactions on, 2015, 64(5):

1204-1214

[22] Grondin J, Grimal Q, Engelke K, et al. Potential of first arriving signal to assess cortical bone geometry at the hip with QUS: a model based study[J]. Ultrasound in medicine & biology, 2010, 36(4): 656-666.

[23] Lee K I. Dependences of ultrasonic properties on the propagation angle with respect to the trabecular alignment in trabecular bone[J]. Journal of the Korean Physical Society, 2014, 64(12): 1802-1807.

[24] Droin P, Berger G, Laugier P. Velocity dispersion of acoustic waves in cancellous bone[J]. Ultrasonics, Ferroelectrics, and Frequency Control, IEEE Transactions on, 1998, 45(3): 581-592.

[25] Wear K. A. The effects of frequency-dependent attenuation and dispersion on sound speed measurements: applications in human trabecular bone[J]. Ultrasonics, Ferroelectrics, and Frequency Control, IEEE Transactions on, 2000, 47(1): 265-273.

[26] Fry F, Barger J. Acoustical properties of the human skull[J]. Journal of the Acoustical Society of America, 1978, 63(5): 1576-1590.

[27] Pal S, Saha S, Reddy G N. Frequency-dependence of ultrasonic characteristic of cancellous bone[C]//Biomaterials Medical Devices and Artificial Organs. 270 Madison AVE, New York, NY 10016: Marcel Dekker INC, 1981, 9(4): 362-363.

[28] Pouet B F, Rasolofosaon N J P. Measurement of broadband intrinsic ultrasonic attenuation and dispersion in solids with laser techniques[J]. The Journal of the Acoustical Society of America, 1993, 93(3): 1286-1292.

[29] Nicholson P H F, Lowet G, Langton C M, et al. A comparison of time-domain and frequency-domain approaches to ultrasonic velocity measurement in trabecular bone[J]. Physics in medicine and biology, 1996, 41(11): 2421.

[30] Bauer A, Marutyan K, Holland M. Negative dispersion in bone: The role of interference in measurements of the apparent phase velocity of two temporally overlapping signals[J]. Journal of the Acoustical Society of America, 2008, 123(4): 2407-2414.

[31] Anderson C C, Bauer A Q, Marutyan K R, et al. Phase velocity of cancellous bone: Negative dispersion arising from fast and slow waves, interference, diffraction, and phase cancellation at piezoelectric receiving elements[M]//Bone Quantitative Ultrasound. Springer Netherlands, 2011: 319-330.

[32] Bogna D, Wojciech P, Jerzy P. Prediction of the biomechanical properties of cancellous bone using ultrasound velocity and bone mineral density[J]. Diagnostics and Medical Technology, 2002; 8(1): 15-20.

[33] Hosokawa A, Otani T. Acoustic anisotropy in bovine cancellous bone[J]. The Journal of the Acoustical Society of America, 1998, 103(5): 2718-2722.

[34] Nicholson P, Muller R, Lowet G. Do quantitative ultrasound measurements reflect structure independently of density in human vertebral cancellous bone?[J]. Bone, 1998, 23(5): 425-431.

[35] Sugita H, Oka M, Toguchida J. Anisotropy of osteoporotic cancellous bone[J]. Bone, 1999, 24(5): 513-516.

[36] Maquer G, Musy S, Wandel J. Bone Volume Fraction and Fabric Anisotropy Are Better Determinants of Trabecular Bone Stiffness Than Other Morphological Variables[J]. Journal of Bone and Mineral Research, 2015, 30(6): 1000-1008.

[37] Sandor T, Felsenberg D, Kalender W A, et al. Global and regional variations in the spinal trabecular bone: single and dual energy examinations[J]. The Journal of Clinical Endocrinology & Metabolism, 1991, 72(5): 1157-1168.

[38] Tassani S, Öhman C, Baleani M, et al. Anisotropy and inhomogeneity of the trabecular structure can describe the mechanical strength of osteoarthritic cancellous bone[J]. Journal of biomechanics, 2010, 43(6): 1160-1166.

[39] Busse B, Hahn M, Soltau M, et al. Increased calcium content and inhomogeneity of mineralization render bone toughness in osteoporosis: mineralization, morphology and biomechanics of human single trabeculae[J]. Bone, 2009, 45(6): 1034-1043.